

---

---

# Prospective Comparison of $^{99m}\text{Tc}$ -MDP Scintigraphy, Combined $^{18}\text{F}$ -NaF and $^{18}\text{F}$ -FDG PET/CT, and Whole-Body MRI in Patients with Breast and Prostate Cancer

Ryogo Minamimoto<sup>1,2</sup>, Andreas Loening<sup>3</sup>, Mehran Jamali<sup>1,2</sup>, Amir Barkhodari<sup>1</sup>, Camila Mosci<sup>1</sup>, Tatianie Jackson<sup>1</sup>, Piotr Obara<sup>3</sup>, Valentina Taviani<sup>3</sup>, Sanjiv Sam Gambhir<sup>1,2</sup>, Shreyas Vasanawala<sup>3</sup>, and Andrei Iagaru<sup>1</sup>

<sup>1</sup>Division of Nuclear Medicine and Molecular Imaging, Department of Radiology, Stanford University, Stanford, California;

<sup>2</sup>Molecular Imaging Program at Stanford, Department of Radiology, Stanford University, Stanford, California; and <sup>3</sup>Radiological Sciences Laboratory, Department of Radiology, Stanford University, Stanford, California

---

We prospectively evaluated the use of combined  $^{18}\text{F}$ -NaF/ $^{18}\text{F}$ -FDG PET/CT in patients with breast and prostate cancer and compared the results with those for  $^{99m}\text{Tc}$ -MDP bone scintigraphy and whole-body MRI. **Methods:** Thirty patients (15 women with breast cancer and 15 men with prostate cancer) referred for standard-of-care bone scintigraphy were prospectively enrolled in this study.  $^{18}\text{F}$ -NaF/ $^{18}\text{F}$ -FDG PET/CT and whole-body MRI were performed after bone scintigraphy. The whole-body MRI protocol consisted of both unenhanced and contrast-enhanced sequences. Lesions detected with each test were tabulated, and the results were compared. **Results:** For extraskelatal lesions,  $^{18}\text{F}$ -NaF/ $^{18}\text{F}$ -FDG PET/CT and whole-body MRI had no statistically significant differences in sensitivity (92.9% vs. 92.9%,  $P = 1.00$ ), positive predictive value (81.3% vs. 86.7%,  $P = 0.68$ ), or accuracy (76.5% vs. 82.4%,  $P = 0.56$ ). However,  $^{18}\text{F}$ -NaF/ $^{18}\text{F}$ -FDG PET/CT showed significantly higher sensitivity and accuracy than whole-body MRI (96.2% vs. 81.4%,  $P < 0.001$ , 89.8% vs. 74.7%,  $P = 0.01$ ) and bone scintigraphy (96.2% vs. 64.6%,  $P < 0.001$ , 89.8% vs. 65.9%,  $P < 0.001$ ) for the detection of skeletal lesions. Overall,  $^{18}\text{F}$ -NaF/ $^{18}\text{F}$ -FDG PET/CT showed higher sensitivity and accuracy than whole-body MRI (95.7% vs. 83.3%,  $P < 0.002$ , 87.6% vs. 76.0%,  $P < 0.02$ ) but not statistically significantly so when compared with a combination of whole-body MRI and bone scintigraphy (95.7% vs. 91.6%,  $P = 0.17$ , 87.6% vs. 83.0%,  $P = 0.53$ ).  $^{18}\text{F}$ -NaF/ $^{18}\text{F}$ -FDG PET/CT showed no significant difference from a combination of  $^{18}\text{F}$ -NaF/ $^{18}\text{F}$ -FDG PET/CT and whole-body MRI. No statistically significant differences in positive predictive value were noted among the 3 examinations. **Conclusion:**  $^{18}\text{F}$ -NaF/ $^{18}\text{F}$ -FDG PET/CT is superior to whole-body MRI and  $^{99m}\text{Tc}$ -MDP scintigraphy for evaluation of skeletal disease extent. Further,  $^{18}\text{F}$ -NaF/ $^{18}\text{F}$ -FDG PET/CT and whole-body MRI detected extraskelatal disease that may change the management of these patients.  $^{18}\text{F}$ -NaF/ $^{18}\text{F}$ -FDG PET/CT provides diagnostic ability similar to that of a combination of whole-body MRI and bone scintigraphy in patients with breast and prostate cancer. Larger cohorts are needed to confirm these preliminary findings, ideally using the newly introduced simultaneous PET/MRI scanners.

**Key Words:**  $^{99m}\text{Tc}$ -MDP;  $^{18}\text{F}$ -NaF;  $^{18}\text{F}$ -FDG; whole-body MRI; prostate cancer; breast cancer

**J Nucl Med 2015; 56:1862–1868**

DOI: 10.2967/jnumed.115.162610

---

**I**n patients with breast cancer, the National Comprehensive Cancer Network guidelines recommend diagnostic CT of the chest and abdomen (and pelvis if needed),  $^{99m}\text{Tc}$ -methylene diphosphonate ( $^{99m}\text{Tc}$ -MDP) bone scintigraphy or  $^{18}\text{F}$ -NaF PET/CT, and optional  $^{18}\text{F}$ -FDG PET/CT (1). Although  $^{18}\text{F}$ -FDG PET/CT has great potential for identifying locally advanced and metastatic lesions (2), the guidelines recommend it only if the results of conventional imaging are equivocal or suggestive. Bone scintigraphy or  $^{18}\text{F}$ -NaF PET/CT may be avoided when  $^{18}\text{F}$ -FDG PET/CT has already identified skeletal metastasis, according to the same guidelines. However, the sensitivity of  $^{18}\text{F}$ -FDG PET/CT for detection of osteoblastic lesions is limited in breast cancer (3).  $^{18}\text{F}$ -FDG PET/CT has not been recommended by the National Comprehensive Cancer Network guidelines for prostate cancer (4), although there are reports suggesting its usefulness in detecting locally recurrent or metastatic disease, assessing the extent of metabolically active, castration-resistant disease (5).  $^{18}\text{F}$ -FDG uptake in prostate cancer lesions is an independent prognostic factor and provides information complementary to that from bone scintigraphy (6).  $^{18}\text{F}$ -NaF PET/CT has greater sensitivity than bone scintigraphy and therefore has been recommended for evaluation of skeletal metastases in patients with prostate cancer (4). Skeletal metastases from prostate cancer are usually osteoblastic but may also have mixed or osteolytic features (7).  $^{18}\text{F}$ -NaF PET/CT is superior to bone scintigraphy for skeletal lesion detection in prostate and breast cancer (8–11).

Whole-body MRI with diffusion-weighted imaging is as sensitive as  $^{18}\text{F}$ -FDG PET/CT but less specific for the detection of locoregional or metastatic breast cancer (12). Whole-body diffusion-weighted imaging has higher specificity but lower sensitivity than  $^{18}\text{F}$ -NaF PET/CT in prostate cancer (13).

The combined administration of  $^{18}\text{F}$ -NaF and  $^{18}\text{F}$ -FDG ( $^{18}\text{F}$ -/ $^{18}\text{F}$ -FDG) in a single PET/CT scan for cancer detection has been advocated for detecting both extraskelatal and skeletal lesions (14,15), and a prospective international multicenter trial showed promising results (16).

---

Received Jun. 23, 2015; revision accepted Sep. 10, 2015.

For correspondence or reprints contact: Andrei Iagaru, Division of Nuclear Medicine and Molecular Imaging, Department of Radiology, Stanford University, 300 Pasteur Dr., H2200, Stanford, CA 94305.

E-mail: aiagaru@stanford.edu

Published online Sep. 24, 2015.

COPYRIGHT © 2015 by the Society of Nuclear Medicine and Molecular Imaging, Inc.

We now evaluated the performance of  $^{18}\text{F}$ - $^{18}\text{F}$ -FDG PET/CT for the detection of extraskelatal and skeletal lesions in a selected population of patients with breast and prostate cancer and compared it with whole-body MRI and bone scintigraphy.

## MATERIALS AND METHODS

### Patient Population

The local Institutional Review Board and Cancer Center Scientific Review Committee approved this study, and all participants gave written informed consent. To be included, patients had to be older than 18 y at the time of recruitment; have a diagnosis of breast cancer with an initial clinical stage of III or more; have a diagnosis of prostate cancer with an initial clinical stage of II or more or a serum prostate-specific antigen level of 10 or more; have been referred for evaluation of possible skeletal metastases with bone scintigraphy or have shown the presence of skeletal metastases on bone scintigraphy; and be able to remain still for the duration of the imaging procedure. Exclusion criteria were limited to pregnancy/nursing and the presence of metallic implants (contraindicated for whole-body MRI).

Between November 2012 and July 2014, 15 women (mean age  $\pm$  SD,  $54.1 \pm 12.6$  y; range, 34–76 y) with pathologically proven breast cancer and 15 men (mean age  $\pm$  SD,  $68.3 \pm 9.4$  y; range, 52–84 y) with pathologically proven prostate cancer were included in this study. Bone scintigraphy was performed first and was followed by the  $^{18}\text{F}$ - $^{18}\text{F}$ -FDG PET/CT and whole-body MRI scans. The interval was  $15.4 \pm 8.0$  d between bone scintigraphy and  $^{18}\text{F}$ - $^{18}\text{F}$ -FDG PET/CT and  $2.5 \pm 3.9$  d between  $^{18}\text{F}$ - $^{18}\text{F}$ -FDG PET/CT and whole-body MRI. At the time of bone scintigraphy, the prostate-specific antigen levels for prostate cancer patients, and the pathologic result for expression of estrogen receptor, progesterone receptor, and human epidermal receptor 2 for breast cancer patients, were recorded.

### Bone Scintigraphy Protocol

No patient preparation was required. Pregnancy was excluded by history. The intravenous dose of  $^{99\text{m}}\text{Tc}$ -MDP was  $935.6 \pm 42.1$  MBq (range, 777.0–1,017.5 MBq). The patients were asked to return to the clinic 3 h after  $^{99\text{m}}\text{Tc}$ -MDP administration, during which time they were encouraged to hydrate and void. On returning, planar images of the whole body and spot views of the thorax and pelvis in anterior and posterior views were acquired. Per routine clinical practice, additional spot (planar or oblique) views of the body were obtained if deemed necessary. The images were acquired using dual-head  $\gamma$ -cameras (Infinia Hawkeye 4 [GE Healthcare] or Skylight [Philips Healthcare]). All images were interpreted using a dedicated Xeleris workstation version 2.0551; GE Healthcare). SPECT or SPECT/CT images were not acquired.

### $^{18}\text{F}$ - $^{18}\text{F}$ -FDG PET/CT Protocol

The patients were scanned on Discovery 600 or 690 scanners (GE Healthcare). There were only small (<10%) differences in SUV measurements between scanners based on data from phantom studies. Patients were asked to fast for 6 h before injection of  $^{18}\text{F}$ - $^{18}\text{F}$ -FDG. For the  $^{18}\text{F}$ - $^{18}\text{F}$ -FDG PET/CT scans, the 2 radiotracers were delivered from the local cyclotron facilities in separate syringes and intravenously administered sequentially, without delay. For all PET/CT scans, total-body (vertex to toes) PET/CT images were obtained in 3-dimensional mode, with the patients' arms at their sides. The PET images were reconstructed with a standard iterative algorithm (ordered-subset expectation maximization, 2 iterative steps and 32 subsets for Discovery 600 and 2 iterative steps and 24 subsets for Discovery 690), as recommended by the manufacturer.

The dosages of  $^{18}\text{F}$ - $^{18}\text{F}$ -FDG were  $567.0 \pm 30.0$  MBq (range, 506.9–625.3 MBq), of which  $^{18}\text{F}$ -FDG included  $370.1 \pm 24.7$  MBq (range,

321.9–414.4 MBq) and  $^{18}\text{F}$ -NaF included  $189.8 \pm 16.1$  MBq (range, 155.4–218.3 MBq). The time from injection to the start of the  $^{18}\text{F}$ - $^{18}\text{F}$ -FDG PET/CT scans was  $70.1 \pm 12.2$  min (range, 50–104 min).

### Whole-Body MRI Protocols and Image Reconstruction

Whole-body MRI studies were acquired on a 750W 3-T scanner (GE Healthcare) using a whole-body coil. Unenhanced sequences included coronal T1-weighted fast spin echo imaging (repetition time/echo time [TR/TE],  $\sim 700/8$  ms; echo train length, 6; bandwidth, 54 kHz; flip angle,  $90^\circ$ ; slice thickness, 8 mm; 0.5 excitations; field of view, 44 cm; matrix,  $448 \times 256$ ), coronal short- $\tau$  inversion recovery imaging (TR/TE, 9,500/45 ms; inversion time, 190 ms; echo train length, 20; bandwidth, 62.5 kHz; slice thickness, 8 mm; field of view, 44 cm; 0.5 excitations; matrix,  $384 \times 224$ ) with station 2 (lungs) acquired in a breath hold (TR/TE, 3,000/45 ms; inversion time, 190 ms; slice thickness, 8 mm; field of view, 44 cm; 0.5 excitations; matrix,  $384 \times 192$ ), and axial echo planar diffusion-weighted imaging (TR/TE, 4,300/55 ms; slice thickness, 8 mm; slice spacing, 8 mm; b value, 50 and 500 ms; field of view, 40 cm; 4 excitations; matrix,  $80 \times 128$ ). After injection of a weight-based dose of gadofosveset (Ablavar; Lantheus Medical Imaging), enhanced sequences were obtained consisting of axial 3-dimensional spoiled gradient recalled echo imaging with 2-point Dixon fat/water separation (flip angle,  $15^\circ$ ; TR/TE, 4.5/1.1 and 2.3 ms; slice thickness, 3 mm; field of view, 44 cm; matrix,  $320 \times 256$ ).

### Image Analysis

The bone scintigraphy and  $^{18}\text{F}$ - $^{18}\text{F}$ -FDG PET/CT scans were interpreted by 2 board-certified nuclear medicine physicians in randomized order, with masking of the diagnosis and the results of other imaging studies. Two board-certified radiologists performed the whole-body MRI interpretation also in randomized order. Agreement was reached by consensus. A direct comparison for each detected lesion was performed among the 3 scans by one of the investigators. For the interpretation of the scans, visual analysis was used instead of semiquantitative analysis (i.e., SUV cutoffs). For the  $^{18}\text{F}$ - $^{18}\text{F}$ -FDG PET/CT scans, areas of focally increased  $^{18}\text{F}$ - $^{18}\text{F}$ -FDG uptake were recorded as malignant unless a benign etiology (e.g., degenerative changes or hemangioma) for this uptake was identified at the same location on the corresponding CT images. The CT component of PET/CT was used to determine whether bone lesions identified on PET had an osteoblastic or osteolytic appearance. For whole-body MRI, all sequences were assessed concurrently, with the radiologist's clinical experience used for detecting lesions. Visual conspicuity against background on the diffusion-weighted images and the presence of an anatomically corresponding abnormality on the fast spoiled gradient-echo and short- $\tau$  inversion recovery images were the criteria for detecting a lesion on whole-body MRI. Diagnostic accuracy was evaluated by comparing the bone scintigraphy,  $^{18}\text{F}$ - $^{18}\text{F}$ -FDG PET/CT, and whole-body MRI results with the final diagnoses as confirmed by histologic evaluation, clinical follow-up, or other imaging studies. We also evaluated the diagnostic ability of combining the results from bone scintigraphy and whole-body MRI and from  $^{18}\text{F}$ - $^{18}\text{F}$ -FDG PET/CT and whole-body MRI.

### Statistical Analysis

Differences in sensitivity and accuracy were compared by the McNemar test. The  $\chi^2$  test for independence was performed to compare the positive predictive value (PPV). The statistical difference of specificity and negative predictive value (NPV) were not tested in this study because of the bias in the population. *P* values of less than 0.05 were considered statistically significant.

## RESULTS

The clinical characteristics of the enrolled patients are shown in Table 1. Two patients with prostate cancer could not complete

**TABLE 1**  
Clinical Characteristics of Patient Population

Characteristic	Female (breast cancer)	Male (prostate cancer)
Number of patients	15	15
Mean age ± SD (y)	54.1 ± 12.6	68.3 ± 9.4
Clinical stage at initial diagnosis		
II	0	5
III	8	4
IV	7	6
Indication for bone scintigraphy		
Initial treatment strategy	3	1
Subsequent treatment strategy	12	14
Prostate-specific antigen		
Mean ± SD		8.6 ± 10.1
Range		0.1–30.3
Pathologic findings		
ER+, PR+, Her2–	5	—
ER+, PR+, Her2+	4	—
ER+, PR–, Her2+	2	—
ER–, PR–, Her2–	2	—
ER–, PR–, Her2+	2	—

ER = estrogen receptor; PR = progesterone receptor; Her2 = human epidermal receptor 2.

the whole-body MRI scan and were therefore excluded from the analysis.

Pathology reports (13% of the patients) or clinical follow-up (87% of the patients) were available as the gold standard for the results. Suspected malignant lesions were identified by  $^{18}\text{F}$ - $^{18}\text{F}$ -FDG PET/CT in 20 of 30 participants (breast cancer:  $n = 12$ , prostate cancer:  $n = 8$ ), by bone scintigraphy in 16 of 30 participants (breast cancer:  $n = 10$ , prostate cancer:  $n = 6$ ), by whole-body MRI in 19 of 28 participants (breast cancer:  $n = 11$ , prostate cancer:  $n = 8$ ), by a combination of whole-body MRI and bone scintigraphy in 19 of 28 participants (breast cancer:  $n = 11$ , prostate cancer:  $n = 8$ ), and by a combination of whole-body MRI and  $^{18}\text{F}$ - $^{18}\text{F}$ -FDG PET/CT in 20 of 28 participants (breast cancer:  $n = 11$ , prostate cancer:  $n = 9$ ). Typical examples are shown in Figures 1–3.

#### Patient-Based Analysis

Table 2 shows the results of the per-patient analysis. Overestimation of clinical staging by  $^{18}\text{F}$ - $^{18}\text{F}$ -FDG PET/CT occurred in 2 participants. One was a case of false-positive findings in the pelvic skeleton in a patient with prostate cancer, and the other was a case of false-positive findings in an axillary lymph node in a patient with breast cancer. Overestimation of clinical stage by whole-body MRI occurred in the patient who had a false-positive axillary

lymph node on  $^{18}\text{F}$ - $^{18}\text{F}$ -FDG PET/CT. Bone scintigraphy failed to identify skeletal lesion in 2 patients, but these were demonstrated on the corresponding whole-body MRI.

#### Lesion-Based Analysis

**Total Lesions.** In total 98 lesions (extraskeletal:  $n = 16$ ; skeletal:  $n = 82$ ) were identified by  $^{18}\text{F}$ - $^{18}\text{F}$ -FDG PET/CT in 30 participants, 79 lesions (extraskeletal:  $n = 15$ ; skeletal:  $n = 64$ ) were identified by whole-body MRI in 28 participants, 53 lesions (all skeletal) were identified by bone scintigraphy in 30 participants, 85 lesions (extraskeletal:  $n = 15$ , skeletal:  $n = 70$ ) were identified by a combination of whole-body MRI and bone scintigraphy in 28 participants, and 96 lesions (extraskeletal:  $n = 17$ ; skeletal:  $n = 79$ ) were identified by a combination of  $^{18}\text{F}$ - $^{18}\text{F}$ -FDG PET/CT and whole-body MRI in 28 participants.

The per-lesion sensitivity, specificity, PPV, NPV, and accuracy of  $^{18}\text{F}$ - $^{18}\text{F}$ -FDG PET/CT, whole-body MRI, bone scintigraphy, and the combination of whole-body MRI and bone scintigraphy are shown in Table 3. For extraskeletal lesions,  $^{18}\text{F}$ - $^{18}\text{F}$ -FDG PET/CT and whole-body MRI had no statistically significant differences in sensitivity ( $P = 1.00$ ), PPV ( $P = 0.32$ ), or accuracy ( $P = 0.56$ ). However,  $^{18}\text{F}$ - $^{18}\text{F}$ -FDG PET/CT showed significantly higher sensitivity and accuracy than whole-body MRI ( $P < 0.001$ ,  $P < 0.02$ ) and bone scintigraphy ( $P < 0.001$ ,  $P < 0.001$ ) for the detection of skeletal lesions. Overall,  $^{18}\text{F}$ - $^{18}\text{F}$ -FDG PET/CT showed higher sensitivity and accuracy than whole-body MRI ( $P < 0.002$ ,  $P < 0.02$ ) but not statistically significantly so when compared with a combination of whole-body MRI and bone scintigraphy ( $P = 0.17$ ,  $P = 0.52$ ).  $^{18}\text{F}$ - $^{18}\text{F}$ -FDG PET/CT showed no difference from a combination of  $^{18}\text{F}$ - $^{18}\text{F}$ -FDG PET/CT and whole-body MRI. No statistically significant differences in PPV were noted among the 3 examinations.

**Skeletal Lesions.** Among 82 skeletal lesions identified on the CT component of PET/CT, 6 were osteolytic; all 6 occurred in patients with breast cancer. The other 76 lesions were osteoblastic. The per-lesion sensitivity, specificity, PPV, NPV, and accuracy of  $^{18}\text{F}$ - $^{18}\text{F}$ -FDG PET/CT, whole-body MRI, bone scintigraphy, and the combination of whole-body MRI and bone scintigraphy for the osteolytic and osteoblastic skeletal lesions are shown in Tables 3 (prostate and breast cancer) and 4 (breast cancer). For osteolytic lesions,  $^{18}\text{F}$ - $^{18}\text{F}$ -FDG PET/CT and whole-body MRI showed higher sensitivity than bone scintigraphy, but no statistical significance was achieved given the small number of lesions.

For osteoblastic lesions,  $^{18}\text{F}$ - $^{18}\text{F}$ -FDG PET/CT had significantly higher sensitivity ( $P < 0.001$ ) and accuracy ( $P < 0.001$ ) than bone scintigraphy.  $^{18}\text{F}$ - $^{18}\text{F}$ -FDG PET/CT had no statistically significant differences in sensitivity ( $P = 0.61$ ) or PPV ( $P = 0.43$ ) but had higher accuracy than whole-body MRI ( $P < 0.05$ ).  $^{18}\text{F}$ - $^{18}\text{F}$ -FDG PET/CT showed no statistically significant difference from a combination of whole-body MRI and bone scintigraphy ( $P = 0.32$ ,  $P = 0.13$ ) but was less sensitive than a combination of  $^{18}\text{F}$ - $^{18}\text{F}$ -FDG PET/CT and whole-body MRI ( $P = 0.01$ ).

**Breast Cancer.** The per-lesion sensitivity, specificity, PPV, NPV, and accuracy of  $^{18}\text{F}$ - $^{18}\text{F}$ -FDG PET/CT, whole-body MRI, bone scintigraphy, and the combination of whole-body MRI and bone scintigraphy are shown in Table 4.  $^{18}\text{F}$ - $^{18}\text{F}$ -FDG PET/CT had no statistically significant differences from whole-body MRI in sensitivity ( $P = 1.00$ ) or accuracy ( $P = 0.56$ ) for extraskeletal lesions.  $^{18}\text{F}$ - $^{18}\text{F}$ -FDG PET/CT had significantly higher sensitivity and accuracy for the detection of skeletal lesions than bone scintigraphy ( $P < 0.001$ ), but not when compared with whole-body MRI

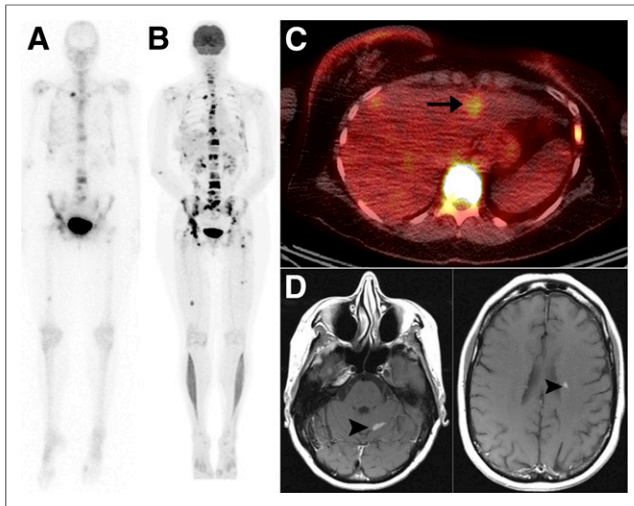


**FIGURE 1.** A 49-year-old woman with breast cancer. (A) Planar whole-body anterior view from  $^{99m}\text{Tc}$ -MDP bone scan and (B) maximum-intensity-projection  $^{18}\text{F}$ - $^{18}\text{F}$ -FDG PET images show multiple bone metastases, more conspicuous on PET. (C) Transaxial fused PET/CT scan demonstrates liver metastasis (arrow). (D) Brain metastases are identified on contrast-enhanced T1-weighted MR images (arrowheads). These were not seen on  $^{18}\text{F}$ - $^{18}\text{F}$ -FDG PET/CT.

( $P = 0.21$ ).  $^{18}\text{F}$ - $^{18}\text{F}$ -FDG PET/CT showed no significant differences from the combination of whole-body MRI and bone scintigraphy ( $P = 1.00$ ). Overall,  $^{18}\text{F}$ - $^{18}\text{F}$ -FDG PET/CT had no significant differences in sensitivity and accuracy from whole-body MRI ( $P = 0.56$ ,  $P = 0.17$ ) or the combination of whole-body MRI and bone scintigraphy ( $P = 0.71$ ,  $P = 0.74$ ).  $^{18}\text{F}$ - $^{18}\text{F}$ -FDG PET/CT had lower sensitivity and accuracy than a combination of results from  $^{18}\text{F}$ - $^{18}\text{F}$ -FDG PET/CT and whole-body MRI ( $P < 0.05$ ). No significant differences in PPV were noted among the 3 examinations.

For osteoblastic lesions,  $^{18}\text{F}$ - $^{18}\text{F}$ -FDG PET/CT had significantly higher sensitivity ( $P < 0.001$ ) and accuracy ( $P < 0.001$ ) than bone scintigraphy.  $^{18}\text{F}$ - $^{18}\text{F}$ -FDG PET/CT had no statistically significant differences in sensitivity ( $P = 0.21$ ) or accuracy ( $P = 0.21$ ) from whole-body MRI.  $^{18}\text{F}$ - $^{18}\text{F}$ -FDG PET/CT showed no statistically significant difference in sensitivity or accuracy from a combination of whole-body MRI and bone scintigraphy ( $P = 1.00$ ,  $P = 1.00$ ) or a combination of  $^{18}\text{F}$ - $^{18}\text{F}$ -FDG PET/CT and whole-body MRI ( $P = 0.08$ ,  $P = 0.08$ ).

**Prostate Cancer.** The per-lesion sensitivity, specificity, PPV, NPV, and accuracy of  $^{18}\text{F}$ - $^{18}\text{F}$ -FDG PET/CT, whole-body MRI, bone scintigraphy, and the combination of whole-body MRI and bone scintigraphy are shown in Table 5. Both  $^{18}\text{F}$ - $^{18}\text{F}$ -FDG PET/CT and whole-body MRI detected additional extraskeletal lesions in 2 patients.  $^{18}\text{F}$ - $^{18}\text{F}$ -FDG PET/CT had significantly higher sensitivity than whole-body MRI ( $P < 0.02$ ) and bone scintigraphy ( $P < 0.03$ ) in the evaluation of skeletal lesions. However,  $^{18}\text{F}$ - $^{18}\text{F}$ -FDG PET/CT had no significant difference in sensitivity from a combination of whole-body MRI and bone scintigraphy ( $P = 0.08$ ). Overall,  $^{18}\text{F}$ - $^{18}\text{F}$ -FDG PET/CT had statistically significant higher sensitivity than whole-body MRI ( $P < 0.02$ ), but not when compared with a combination of whole-body MRI and bone scintigraphy ( $P = 0.08$ ) or  $^{18}\text{F}$ - $^{18}\text{F}$ -FDG PET/CT and whole-body MRI ( $P = 1.00$ ). No statistically significant differences in PPV were identified between these examinations.

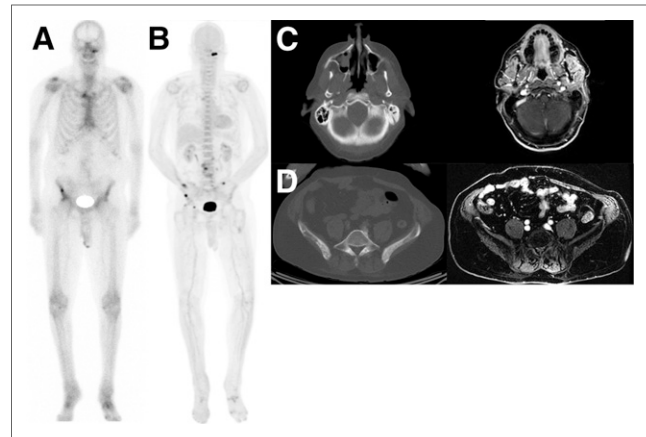


**FIGURE 2.** A 70-year-old man with prostate cancer. (A and B) Planar whole-body anterior view from  $^{99m}\text{Tc}$ -MDP bone scan (A) and maximum-intensity-projection  $^{18}\text{F}$ - $^{18}\text{F}$ -FDG PET images (B) show bone metastases in skull base and right iliac bone, more conspicuous on PET. (C) Skull base lesion was not identified prospectively on CT or contrast-enhanced T1-weighted MRI. (D) Right iliac bone lesion was not identified prospectively on CT or contrast-enhanced T1-weighted MRI.

## DISCUSSION

Our study suggests that PET/CT done after administration of  $^{18}\text{F}$ -NaF and  $^{18}\text{F}$ -FDG followed by a single PET/CT scan has higher accuracy than whole-body MRI and bone scintigraphy for evaluation of the extent of disease in this population of patients with breast and prostate cancer.  $^{18}\text{F}$ - $^{18}\text{F}$ -FDG PET/CT performed as well as a combination of whole-body MRI and bone scintigraphy; therefore, it may serve as a one-stop shop in the imaging management of patients with certain cancers.

Although  $^{18}\text{F}$ -FDG PET/CT can provide high diagnostic accuracy in both the initial and recurrent breast cancer settings compared with conventional imaging (17–19), it has several limitations for the diagnosis of patients with prostate cancer (5).  $^{18}\text{F}$ -FDG PET/CT is also

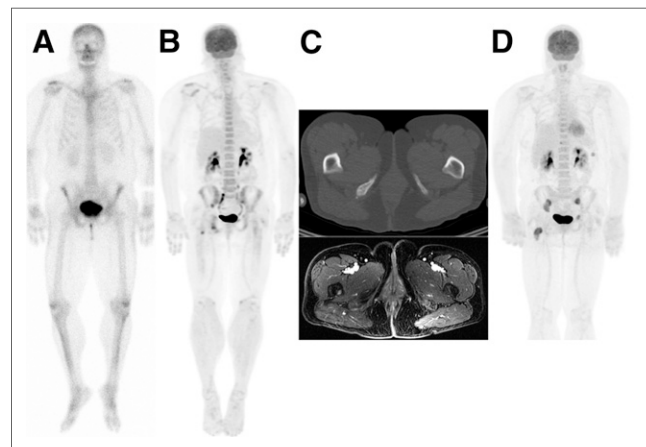


**FIGURE 3.** A 53-year-old woman with breast cancer. (A and B) Planar whole-body anterior view from  $^{99m}\text{Tc}$ -MDP bone scan (A) is negative for bone metastases, whereas maximum-intensity-projection  $^{18}\text{F}$ - $^{18}\text{F}$ -FDG PET images (B) show bone metastases in multiple locations, including right femur. (C) Proximal right femur metastasis was not identified prospectively on CT or contrast-enhanced T1-weighted MRI. (D) Maximum-intensity projection from follow-up  $^{18}\text{F}$ - $^{18}\text{F}$ -FDG PET done 6 mo later demonstrates progression of bone metastases, including in right femur.

**TABLE 2**  
Results of Per-Patient Analysis

Parameter	Examination	Correct	Overestimate	Underestimate
Skeletal lesions	<sup>18</sup> F-/ <sup>18</sup> F-FDG PET/CT	29 (27)	1 (1)	0 (0)
	Whole-body MRI	26	0	0
	Bone scintigraphy	28 (26)	0 (0)	2 (2)
	Bone scintigraphy + whole-body MRI	27	1	0
	<sup>18</sup> F-/ <sup>18</sup> F-FDG PET/CT + whole-body MRI	26	2	0
Clinical staging	<sup>18</sup> F-/ <sup>18</sup> F-FDG PET/CT	28 (26)	2 (2)	0 (0)
	Whole-body MRI	26	2	0
	Bone scintigraphy + whole-body MRI	26	2	0
	<sup>18</sup> F-/ <sup>18</sup> F-FDG PET/CT + whole-body MRI	25	3	0

Number in parenthesis is result based on 28 patients who had whole-body MRI scan.

not recommended for the detection of osteoblastic skeletal lesions (3,20). <sup>18</sup>F-NaF PET/CT is superior to bone scintigraphy and <sup>18</sup>F-FDG PET/CT for the detection of osteoblastic metastases (21). Another study showed that whole-body MRI with diffusion-weighted

imaging had results similar to <sup>18</sup>F-NaF PET/CT in breast cancer and superior to bone scintigraphy (22). The combined <sup>18</sup>F-/<sup>18</sup>F-FDG PET/CT scan can increase sensitivity in the detection of osseous lesions compared with <sup>18</sup>F-FDG PET/CT (14–16,23).

**TABLE 3**  
Per-Lesion Analysis (Breast and Prostate Cancers)

Lesion type	Examination	Sensitivity	Specificity	PPV	NPV	Accuracy
Extraskeletal lesions	<sup>18</sup> F-/ <sup>18</sup> F-FDG PET/CT	92.9	0.0	81.3	0.0	76.5
	Whole-body MRI	92.9	33.3	86.7	50.0	82.4
	<sup>18</sup> F-/ <sup>18</sup> F-FDG PET/CT + whole-body MRI	100.0	0.0	82.4	NA	82.4
Skeletal lesions	<sup>18</sup> F-/ <sup>18</sup> F-FDG PET/CT	96.2 <sup>††</sup>	33.3	93.7	50.0	89.8 <sup>‡§</sup>
	Whole-body MRI	81.4	22.2	89.1	13.3	74.7
	Bone scintigraphy	64.6	77.8	96.2	20.0	65.9
	Bone scintigraphy + whole-body MRI	91.4	22.2	90.1	25.0	83.5
	<sup>18</sup> F-/ <sup>18</sup> F-FDG PET/CT + whole-body MRI	100.0	0.0	89.8	NA	89.8
Osteolytic lesions	<sup>18</sup> F-/ <sup>18</sup> F-FDG PET/CT	100.0	0.0	83.3	NA	83.3
	Whole-body MRI	100.0	0.0	83.3	NA	83.3
	Bone scintigraphy	80.0	100.0	100.0	50.0	83.3
	Bone scintigraphy + whole-body MRI	100.0	0.0	83.3	NA	83.3
	<sup>18</sup> F-/ <sup>18</sup> F-FDG PET/CT + whole-body MRI	100.0	0.0	83.3	NA	83.3
Osteoblastic lesions	<sup>18</sup> F-/ <sup>18</sup> F-FDG PET/CT	95.9 <sup>††  </sup>	37.5	93.4	50.0	90.2 <sup>§¶</sup>
	Whole-body MRI	80.0	25.0	89.7	13.3	74.0
	Bone scintigraphy	63.5	75.0	95.9	18.2	64.6
	Bone scintigraphy + whole-body MRI	90.8	25.0	90.8	25.0	83.6
	<sup>18</sup> F-/ <sup>18</sup> F-FDG PET/CT + whole-body MRI	100.0	0.0	90.2	NA	90.2
Total lesions	<sup>18</sup> F-/ <sup>18</sup> F-FDG PET/CT	95.7 <sup>#</sup>	25.0	90.8	42.9	87.6 <sup>**</sup>
	Whole-body MRI	83.3	25.0	88.6	17.6	76.0
	Bone scintigraphy + whole-body MRI	91.6	25.0	89.5	30.0	83.3
	<sup>18</sup> F-/ <sup>18</sup> F-FDG PET/CT + whole-body MRI	100.0	0.0	87.5	NA	87.5

NA = not applicable. <sup>18</sup>F-/<sup>18</sup>F-FDG PET/CT showed significantly higher sensitivity (<sup>\*</sup>*P* < 0.001, <sup>#</sup>*P* < 0.002) and accuracy (<sup>†</sup>*P* < 0.02, <sup>\*\*</sup>*P* < 0.02, <sup>¶</sup>*P* < 0.05) than whole-body MRI. <sup>18</sup>F-/<sup>18</sup>F-FDG PET/CT showed higher sensitivity (<sup>†</sup>*P* < 0.001) and accuracy (<sup>§</sup>*P* < 0.001) than bone scintigraphy. <sup>18</sup>F-/<sup>18</sup>F-FDG PET/CT showed lower sensitivity than combination of <sup>18</sup>F-/<sup>18</sup>F-FDG PET/CT and whole-body MRI (<sup>||</sup>*P* = 0.01).

**TABLE 4**  
Per-Lesion Analysis (Breast Cancer)

Lesion type	Examination	Sensitivity	Specificity	PPV	NPV	Accuracy
Extraskeletal lesions	<sup>18</sup> F-/ <sup>18</sup> F-FDG PET/CT	91.7	0.0	78.6	0.0	73.3
	Whole-body MRI	91.7	33.3	84.6	50.0	80.0
	<sup>18</sup> F-/ <sup>18</sup> F-FDG PET/CT + whole-body MRI	100.0	0.0	80.0	NA	80.0
Skeletal lesions	<sup>18</sup> F-/ <sup>18</sup> F-FDG PET/CT	93.6*	0.0	91.7	0.0	86.3 <sup>†</sup>
	Whole-body MRI	85.1	0.0	90.9	0.0	78.4
	Bone scintigraphy	53.2	50.0	92.6	8.3	52.9
	Bone scintigraphy + whole-body MRI	93.6	0.0	91.7	0.0	86.3
	<sup>18</sup> F-/ <sup>18</sup> F-FDG PET/CT + whole-body MRI	100.0	0.0	92.2	NA	92.2
Osteolytic lesions	<sup>18</sup> F-/ <sup>18</sup> F-FDG PET/CT	100.0	0.0	83.3	NA	83.3
	Whole-body MRI	100.0	0.0	83.3	NA	83.3
	Bone scintigraphy	80.0	100.0	100.0	50.0	83.3
	Bone scintigraphy + whole-body MRI	100.0	0.0	83.3	NA	83.3
	<sup>18</sup> F-/ <sup>18</sup> F-FDG PET/CT + whole-body MRI	100.0	0.0	83.3	NA	83.3
Osteoblastic lesions	<sup>18</sup> F-/ <sup>18</sup> F-FDG PET/CT	92.9*	0.0	92.9	0.0	86.7 <sup>‡</sup>
	Whole-body MRI	83.3	0.0	92.1	0.0	77.8
	Bone scintigraphy	50.0	33.3	91.3	4.5	48.9
	Bone scintigraphy + whole-body MRI	92.9	0.0	92.9	0.0	86.7
	<sup>18</sup> F-/ <sup>18</sup> F-FDG PET/CT + whole-body MRI	100.0	0.0	93.3	NA	93.3
Total lesions	<sup>18</sup> F-/ <sup>18</sup> F-FDG PET/CT	93.2 <sup>‡</sup>	0.0	88.7	0.0	83.3 <sup>§</sup>
	Whole-body MRI	86.4	14.3	89.5	11.1	78.8
	Bone scintigraphy + whole-body MRI	93.2	14.3	90.2	20.0	84.8
	<sup>18</sup> F-/ <sup>18</sup> F-FDG PET/CT + whole-body MRI	100.0	0.0	89.4	0.0	89.4

NA = not applicable. <sup>18</sup>F-/<sup>18</sup>F-FDG PET/CT showed higher sensitivity (\**P* < 0.001) and accuracy (<sup>†</sup>*P* < 0.001) than bone scintigraphy. <sup>18</sup>F-/<sup>18</sup>F-FDG PET/CT showed lower sensitivity (<sup>‡</sup>*P* < 0.05) and accuracy (<sup>§</sup>*P* < 0.05) than combination of results from <sup>18</sup>F-/<sup>18</sup>F-FDG PET/CT and whole-body MRI.

**TABLE 5**  
Per-Lesion Analysis (Prostate Cancer)

Lesion type	Examination	Sensitivity	Specificity	PPV	NPV	Accuracy
Extraskeletal lesions	<sup>18</sup> F-/ <sup>18</sup> F-FDG PET/CT	100.0	NA	100.0	NA	100.0
	Whole-body MRI	100.0	NA	100.0	NA	100.0
	<sup>18</sup> F-/ <sup>18</sup> F-FDG PET/CT + whole-body MRI	100.0	NA	100.0	NA	100.0
Skeletal lesions (osteoblastic)	<sup>18</sup> F-/ <sup>18</sup> F-FDG PET/CT	100.0 <sup>†</sup>	60.0	94.1	100.0	94.6
	Whole-body MRI	65.4	40.0	85.0	25.0	61.3
	Bone scintigraphy	81.3	100.0	100.0	45.5	83.8
	Bone scintigraphy + whole-body MRI	100.0	40.0	88.5	100.0	89.3
	<sup>18</sup> F-/ <sup>18</sup> F-FDG PET/CT + whole-body MRI	100.0	0.0	82.1	NA	82.1
Total lesions	<sup>18</sup> F-/ <sup>18</sup> F-FDG PET/CT	100.0 <sup>‡</sup>	60.0	94.4	100.0	94.9
	Whole-body MRI	76.0	40.0	86.4	25.0	70.0
	Bone scintigraphy + whole-body MRI	100.0	40.0	89.3	100.0	90.0
	<sup>18</sup> F-/ <sup>18</sup> F-FDG PET/CT + whole-body MRI	100.0	0.0	83.3	NA	83.3

NA = not applicable. <sup>18</sup>F-/<sup>18</sup>F-FDG PET/CT showed significantly higher sensitivity than whole-body MRI (\**P* < 0.02) and bone scintigraphy (<sup>†</sup>*P* < 0.03) in evaluation of skeletal lesions. <sup>18</sup>F-/<sup>18</sup>F-FDG PET/CT showed statistically significant higher sensitivity than whole-body MRI (<sup>‡</sup>*P* < 0.02)

Whole-body MRI detected brain metastases that were missed on  $^{18}\text{F}$ - $^{18}\text{F}$ -FDG PET/CT because of high physiologic  $^{18}\text{F}$ -FDG uptake in the normal cerebral cortex. Therefore, whole-body MRI may be able to provide complementary information in areas where  $^{18}\text{F}$ -FDG PET/CT has known limitations in diagnosis.

Hybrid PET/MRI has recently been introduced clinically. Compared with PET/CT, PET/MRI has advantages due to the better soft-tissue contrast of MRI (24,25). PET and MRI provide complementary information, as they evaluate different biologic processes (26). Therefore, simultaneous  $^{18}\text{F}$ - $^{18}\text{F}$ -FDG PET/MRI may provide more accurate diagnostic performance in patients with breast and prostate cancer.

Limitations of this study include the relatively small number of participants, variations in injected dosage, variations in the time from injection to imaging, and lack of semiquantitative measurements such as SUV. The optimal ratio of  $^{18}\text{F}$ -NaF to  $^{18}\text{F}$ -FDG in the  $^{18}\text{F}$ - $^{18}\text{F}$ -FDG PET/CT scan is also known to be an issue for this approach to imaging cancer patients (27).

## CONCLUSION

$^{18}\text{F}$ - $^{18}\text{F}$ -FDG PET/CT and whole-body MRI are superior to  $^{99\text{m}}\text{Tc}$ -MDP scintigraphy for evaluation of the extent of skeletal disease, as expected from already published data. Further, PET/CT and whole-body MRI detected extraskeletal disease that may change the management of these patients.  $^{18}\text{F}$ - $^{18}\text{F}$ -FDG PET/CT provides diagnostic ability similar to that of a combination of whole-body MRI and bone scintigraphy in patients with breast and prostate cancer. Larger cohorts are needed to confirm these preliminary findings, ideally using the newly introduced simultaneous PET/MRI scanners.

## DISCLOSURE

The costs of publication of this article were defrayed in part by the payment of page charges. Therefore, and solely to indicate this fact, this article is hereby marked "advertisement" in accordance with 18 USC section 1734. GE Healthcare provided financial support for the study; the authors had control of the data and information submitted for publication. No other potential conflict of interest relevant to this article was reported.

## ACKNOWLEDGMENTS

We thank our research coordinators, Frederick Chin, PhD, the staff at the Lucas Cyclotron, and the technologists in the Division of Nuclear Medicine and Molecular Imaging. Special thanks are extended to all our patients and their families.

## REFERENCES

1. Gradishar WJ, Anderson BO, Balassanian R, et al. Breast cancer, version 2.2015. *J Natl Compr Canc Netw*. 2015;13:448–475.
2. Eubank WB, Mankoff D, Bhattacharya M, et al. Impact of FDG PET on defining the extent of disease and on the treatment of patients with recurrent or metastatic breast cancer. *AJR*. 2004;183:479–486.
3. Nakai T, Okuyama C, Kubota T, et al. Pitfalls of FDG-PET for the diagnosis of osteoblastic bone metastases in patients with breast cancer. *Eur J Nucl Med Mol Imaging*. 2005;32:1253–1258.
4. Mohler JL, Kantoff PW, Armstrong AJ, et al. Prostate cancer, version 2.2014. *J Natl Compr Canc Netw*. 2014;12:686–718.

5. Jadvar H. Molecular imaging of prostate cancer with  $^{18}\text{F}$ -fluorodeoxyglucose PET. *Nat Rev Urol*. 2009;6:317–323.
6. Meirelles GS, Schoder H, Ravizzini GC, et al. Prognostic value of baseline [ $^{18}\text{F}$ ] fluorodeoxyglucose positron emission tomography and  $^{99\text{m}}\text{Tc}$ -MDP bone scan in progressing metastatic prostate cancer. *Clin Cancer Res*. 2010;16:6093–6099.
7. Koutsilieris M, Rabbani SA, Bennett HP, Goltzman D. Characteristics of prostate-derived growth factors for cells of the osteoblast phenotype. *J Clin Invest*. 1987;80:941–946.
8. Even-Sapir E, Metser U, Mishani E, Lievshitz G, Lerman H, Leibovitch I. The detection of bone metastases in patients with high-risk prostate cancer:  $^{99\text{m}}\text{Tc}$ -MDP planar bone scintigraphy, single- and multi-field-of-view SPECT,  $^{18}\text{F}$ -fluoride PET, and  $^{18}\text{F}$ -fluoride PET/CT. *J Nucl Med*. 2006;47:287–297.
9. Ben-Haim S, Israel O. Breast cancer: role of SPECT and PET in imaging bone metastases. *Semin Nucl Med*. 2009;39:408–415.
10. Iagaru A, Mitra E, Dick DW, Gambhir SS. Prospective evaluation of  $^{99\text{m}}\text{Tc}$  MDP scintigraphy,  $^{18}\text{F}$  NaF PET/CT, and  $^{18}\text{F}$  FDG PET/CT for detection of skeletal metastases. *Mol Imaging Biol*. 2012;14:252–259.
11. Withofs N, Grayet B, Tancredi T, et al.  $^{18}\text{F}$ -fluoride PET/CT for assessing bone involvement in prostate and breast cancers. *Nucl Med Commun*. 2011;32:168–176.
12. Heusner TA, Kuemmel S, Koeninger A, et al. Diagnostic value of diffusion-weighted magnetic resonance imaging (DWI) compared to FDG PET/CT for whole-body breast cancer staging. *Eur J Nucl Med Mol Imaging*. 2010;37:1077–1086.
13. Mosavi F, Johansson S, Sandberg DT, Turesson I, Sorensen J, Ahlstrom H. Whole-body diffusion-weighted MRI compared with  $^{18}\text{F}$ -NaF PET/CT for detection of bone metastases in patients with high-risk prostate carcinoma. *AJR*. 2012;199:1114–1120.
14. Iagaru A, Mitra E, Yaghoubi SS, et al. Novel strategy for a cocktail  $^{18}\text{F}$ -fluoride and  $^{18}\text{F}$ -FDG PET/CT scan for evaluation of malignancy: results of the pilot-phase study. *J Nucl Med*. 2009;50:501–505.
15. Lin FI, Rao JE, Mitra ES, et al. Prospective comparison of combined  $^{18}\text{F}$ -FDG and  $^{18}\text{F}$ -NaF PET/CT vs.  $^{18}\text{F}$ -FDG PET/CT imaging for detection of malignancy. *Eur J Nucl Med Mol Imaging*. 2012;39:262–270.
16. Iagaru A, Mitra E, Mosci C, et al. Combined  $^{18}\text{F}$ -fluoride and  $^{18}\text{F}$ -FDG PET/CT scanning for evaluation of malignancy: results of an international multicenter trial. *J Nucl Med*. 2013;54:176–183.
17. Radan L, Ben-Haim S, Bar-Shalom R, Guralnik L, Israel O. The role of FDG-PET/CT in suspected recurrence of breast cancer. *Cancer*. 2006;107:2545–2551.
18. Rosen EL, Eubank WB, Mankoff DA. FDG PET, PET/CT, and breast cancer imaging. *Radiographics*. 2007;27(suppl 1):S215–S229.
19. Dirisamer A, Halpern BS, Flory D, et al. Integrated contrast-enhanced diagnostic whole-body PET/CT as a first-line restaging modality in patients with suspected metastatic recurrence of breast cancer. *Eur J Radiol*. 2010;73:294–299.
20. Uematsu T, Yuen S, Yukisawa S, et al. Comparison of FDG PET and SPECT for detection of bone metastases in breast cancer. *AJR*. 2005;184:1266–1273.
21. Hsu WK, Virk MS, Feeley BT, Stout DB, Chatziioannou AF, Lieberman JR. Characterization of osteolytic, osteoblastic, and mixed lesions in a prostate cancer mouse model using  $^{18}\text{F}$ -FDG and  $^{18}\text{F}$ -fluoride PET/CT. *J Nucl Med*. 2008;49:414–421.
22. Yoon SH, Kim KS, Kang SY, et al. Usefulness of  $^{18}\text{F}$ -fluoride PET/CT in breast cancer patients with osteosclerotic bone metastases. *Nucl Med Mol Imaging*. 2013;47:27–35.
23. Minamimoto R, Mosci C, Jamali M, et al. Semiquantitative analysis of the biodistribution of the combined  $^{18}\text{F}$ -NaF and  $^{18}\text{F}$ -FDG administration for PET/CT imaging. *J Nucl Med*. 2015;56:688–694.
24. Iagaru A, Mitra E, Minamimoto R, et al. Simultaneous whole-body time-of-flight  $^{18}\text{F}$ -FDG PET/MRI: a pilot study comparing SUVmax with PET/CT and assessment of MR image quality. *Clin Nucl Med*. 2015;40:1–8.
25. Antoch G, Bockisch A. Combined PET/MRI: a new dimension in whole-body oncology imaging? *Eur J Nucl Med Mol Imaging*. 2009;36(suppl 1):S113–S120.
26. Kwee TC, Takahara T, Ochiai R, et al. Complementary roles of whole-body diffusion-weighted MRI and  $^{18}\text{F}$ -FDG PET: the state of the art and potential applications. *J Nucl Med*. 2010;51:1549–1558.
27. Richmond K, McLean N, Rold T, Szczodroski A, Dresser T, Hoffman T. Optimizing a F-18 NaF and FDG cocktail as a preclinical cancer screening tool for molecular imaging [abstract]. *J Nucl Med*. 2011;52(suppl 1):2455.